

Study on Collapse Evaluation Method for RC Buildings Considering Redundant Failure Behaviour

Satoshi Komatsu¹, Mari Funayama², Zazirej Stanislav¹, Akira Hosoda¹ and Kuniyoshi Sugimoto¹

1. Institute of Urban Innovation, Yokohama National University, 79-5 Tokiwadai, Hodogaya, Yokohama (240-8501), JAPAN

2. Graduate School of Urban Innovation, Yokohama National University, 79-5 Tokiwadai, Hodogaya, Yokohama (240-8501), JAPAN

Summary

Accurately assessing the collapse potential of buildings is very important in Japan, a country prone to large earthquakes, to ensure the protection of human lives. This study evaluates the applicability of numerical simulation by analysing the behaviour of a full-scale 6-story RC building subjected to actual earthquake motion. Additionally, for column members that collapsed due to shear failure, an index based on the amount of deformation characteristics before and after seismic damage was applied to assess the reduction in load-carrying capacity. The results indicate that the nonlinear behaviour of RC buildings can be estimated with high accuracy when the physical properties of concrete are appropriately set. Furthermore, the proposed indices were found to be capable of accurately evaluating the damage conditions leading to a reduction in the load-carrying capacity of members.

1 DEMAND FOR MORE ADVANCED SEISMIC PERFORMANCE EVALUATION METHODS

Japan experiences earthquakes more frequently than most other countries, making it is a critical responsibility for engineers to ensure that human lives and property are protected from seismic damage. The Ministry of Education, Culture, Sports, Science and Technology [1] has updated its seismic intensity prediction maps, which show the probability of strong earthquakes in the future. According to these maps, the probability of an earthquake of intensity 6- or greater occurring within the next 30 years from 2020 is particularly high along the Pacific coast of Japan and in the Tokyo metropolitan area, ranging from 26% to nearly 100%. This high probability is due to the presence of plate boundaries off the Pacific coast between the land and the sea that cause trench-type earthquakes along the Kuril Trench, the Japan Trench, and the Nankai Trough, among other areas. The probability is so high because the recurrence interval of these trench-type earthquakes is relatively short, typically ranging from several decades to around 100 years.

We will examine two typical examples of reinforced concrete structure collapse due to earthquakes. The first is collapse of the first floor of a building with a piloti structure. In some cases, buildings used as shops, offices, garages, or warehouses do not have load-bearing walls on the first floor to maximize interior space. In such cases, the rigidity and load-bearing capacity of the first floor is lower compared to the upper floors, causing large plastic deformation to concentrate on the first floor, and ultimately leading to collapse of that floor. This vulnerability is particularly evident in buildings constructed before 1971, where many columns lacked effective shear reinforcement, resulting in numerous first floor failures. Although rare, some buildings have also collapsed sideways due an unfavourable structural centre of gravity, as shown in Figure 1.

The second typical example of reinforced concrete structure collapse is the failure of intermediate floors. There have been reports of intermediate floor collapse in buildings where the structural type was switched from steel-framed reinforced concrete to reinforced concrete, in buildings where seismic

reinforcement work was completed on lower floors, causing weakness in the floor directly above, in buildings where the number of bearing walls was reduced, in building floors where the cross-section of the columns was significantly reduced, in building floors where vertical setbacks were introduced, and in building floors where torsional vibration was induced due to the uneven distribution of bearing walls. Figure 2 shows a typical case of intermediate-floor collapse that occurred in the 2016 Kumamoto earthquake. Note that this type of collapse has not been observed in buildings constructed after 1981, following revision of design methodologies.

To prevent damage such as described above, it is important to develop numerical simulation technology capable of accurately predicting building collapse behaviour under anticipated seismic motion, and to set appropriate limit values based on well-defined indices for ensuring required structural performance of each building. In this study, we confirmed the applicability of the material nonlinear finite element method (FEM) program that the authors have been involved in developing to the results of earthquake response analysis of buildings. Furthermore, we propose a method for rationally evaluating the risk of building collapse due to damage to wall and column members by focusing on the relative deformation amount within these members.



Fig. 1 Building that collapsed sideways and blocked the road [2]



Fig. 2 City Hall Main Building with intermediate-story collapse [3]

2 OVERVIEW OF THE SHAKING TABLE TEST ON A FULL-SCALE 6-STORY REINFORCED CONCRETE BUILDING

In this study, we analysed the results of a shaking table test conducted on a full-scale 6-story reinforced concrete building with seismic walls [4]. The test was conducted at the Full-Scale 3D Earthquake Simulation Facility of the National Research Institute for Earth Science and Disaster Prevention.

Figure 3 presents the plan and frame diagram of the test building. It is a 6-story reinforced concrete seismic wall frame structure with 3 spans in the longitudinal direction (Y direction) and 2 spans in the direction perpendicular to that (X direction). The span length in both the X and Y directions is 5000 mm, and each floor has a height of 500 mm, for a total building height of 16200 mm. The cross-sectional sizes of the members are the same on each floor: main columns 500×500 mm, intermediate columns 300×300 mm, main beams (G1, G2) 300×500 mm, and secondary beams 200×400 mm. The reinforcement details of each component are as follows: the main reinforcement of the columns on each floor is 8-D19, with 2-D10 at 100 mm spacing; the seismic walls (SW1) are 150 mm thick, reinforced with double D10@300 mm spacing both vertically and horizontally, with the exception of some parts; the upper reinforcement of the main beams (G1, G2) is 3-D19, the lower reinforcement is 2-D19, and the stirrups are 2-D10 at 200 mm spacing. The design standard strength of the concrete was set at 18 N/mm^2 . However, according to reference [4], the compressive strength of the concrete test pieces cured in water at the construction site on the day of the shaking table test was 31.7, 30.7, 28.2, 27.3, 25.2, and 22.8 MPa for the first to sixth floors, respectively. The yield strength of the rebar was 398 MPa for D19 and 369 MPa for D10. The weight of each floor is approximately 1.25 MN, and the total weight of the upper part of the first floor columns was 7.50 MN.

The input seismic wave used in the test was observed at the Kobe Marine Observatory of the Japan Meteorological Agency during the Great Hanshin-Awaji Earthquake. The amplitude multiplier was increased in steps of 5%, 10%, 25%, 50%, and 100%, and finally a waveform simulating an aftershock was input at 60%. The building collapsed when the amplitude multiplier reached 60%. The vibration direction was in three directions: two horizontal directions (X and Y) and the vertical direction. The original wave was rotated 45 degrees, and the N45W direction was set as the Y direction of the building, and N45E as the X direction. The final design was such that the test building would collapse in the Y direction.

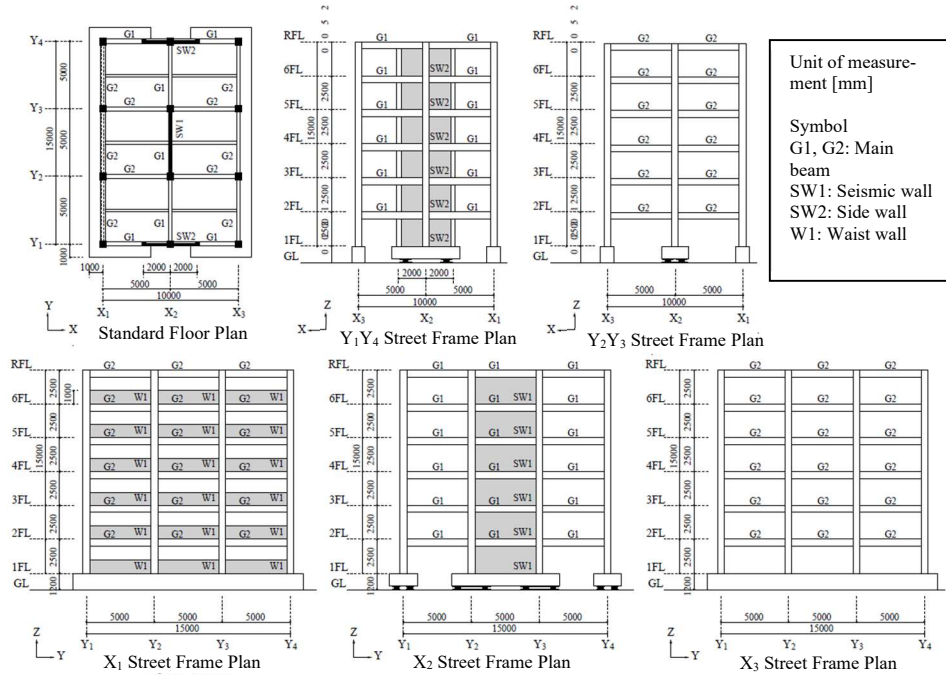


Fig. 3 Floor plan and frame diagram of the test building

3 OVERVIEW OF NUMERICAL SIMULATION

A nonlinear finite element method (FEM) analysis of the material was conducted using the analysis code COM3 [5] for the full-scale experiment described in Chapter 2. The mechanical constitutive model for concrete incorporates one-dimensional compression, tension, and shear transfer on the crack surface, and time dependence is considered for each. In this study, a multi-directional non-orthogonal fixed crack model was selected as the finite element model, taking into account the deformation of the crack surface, which has a dominant effect on the nonlinearity of the element. After crack formation, the tension stiffening model, which takes into account the adhesion effect of the steel bars in the tensile region of the reinforced concrete in a spatially averaged manner, was used. To efficiently and accurately calculate the overall response of the full-scale building, both a distributed crack model and a distributed steel bar model are used. The analysis model was constructed based on previous research [6], and comprised 88,573 elements and 131,024 nodes.

The material properties used in the analysis were based on the experimental values. The rebar diameters used were D19 and D10, and the rebar was arranged in the same way as in the experiment. The compressive strength was based on the values obtained in the experiment for each floor. In addition, the Young's modulus and tensile strength were calculated using the design formula from the Standard Specifications for Concrete [7] to account for drying shrinkage, and then reduced by 20% and 40%, respectively [8].

The analysis model was fed the Kobe Marine Observatory observation wave, which is the same seismic wave as the experiment, as acceleration. The 5% amplitude multiplier was omitted because it

was considered to have minimal impact, and the input was incrementally increased to 10%, 25%, 50%, and 100%. In the X and Y directions, the N45N and N45W components of the measured wave output in the experiment were input to the analysis model. In the Z direction, the UD component of the observed seismic wave was used.

4 DAMAGE ASSESSMENT OF COLUMN MEMBERS

As discussed in Chapter 1, the collapse of the building was caused by the reduction of axial force in the column members. To ensure both safety and rational design, the authors propose that an evaluation index for column members that also takes into account the redundancy of the structure is useful. Therefore, in this study, we verified whether the evaluation method described in seismic performance verification guidelines for underground box culverts at nuclear power plants [8] can be applied to buildings. The structural performance requirement in these guidelines allows for some damage but ensures that the entire structure does not collapse due to an earthquake. Since this aligns with the purpose of this study, we attempted to apply this methodology. The two indices used in the evaluation are “thickness increment of RC member” and “relative displacement on compressive edge in RC member”, and both focus on the amount of relative deformation within the member. The details of these indices are described later, but as summarized in Table 1, the combination of these two indices has been confirmed to be applicable to all cases, such as in-plane or out-of-plane, bending or shear failure, for wall or column members. Furthermore, it has been confirmed to allow the effective assessment of axial force retention in members, ensuring they maintain at least 90% of their force, while also minimizing sensitivity to element length [9].

Table 1 Indices for seismic performance verification of columns or wall members

	Crack type	Failure mode	Indices
Out of plane	Shear cracks	Diagonal tensile failure	“Thickness increment of RC member” and “relative displacement on compressive edge in RC member”
In plane		Shear compressive failure	
Out of plane	Bending cracks	Bending compressive failure	Relative displacement on compressive edge in RC member

4.1 Thickness increment of RC member

The thickness increment of RC member index, which indicates the amount of expansion in the thickness direction of the member, as shown in Eq. (1), is mainly composed of diagonal cracks (X-shaped cracks) and bond splitting cracks, and roughly corresponds to the total of those openings. This index can be applied to both one-way and repetitive loadings.

$$\Delta D_{lim} = \max\{5, 2.5p_w D\} \quad (1)$$

where ΔD_{lim} is the limit value of thickness increment of the RC member [mm], p_w is the shear reinforcement ratio, and D is the member thickness [mm]. Figure 4 shows an image of the nodes used in the calculation. The thickness increment of RC member index is effective for evaluating out-of-plane shear failure because it does not detect the opening of bending cracks but detects the opening of diagonal shear cracks. In this study, relative displacement was calculated between element nodes at the same elevation, and the maximum value was adopted for evaluation. The first term (5 mm) focuses on members without out-of-plane shear reinforcing bars. According to previous experiments with member thicknesses of 400 mm to 800 mm and axial force ratio of -0.05 to 0.05 , the residual load carrying capacity rate in the direction perpendicular to the member axis is 60% to 95% when there is expansion of 5 mm in the thickness direction. The second term ($2.5p_w D$) accounts for the distribution of cracks in members due to the use of shear reinforcing bars. Analytical case studies further confirmed that the relationship shown in Eq. (2) was found across members with different specimen lengths, rebar ratios, and rebar diameters.

$$\varepsilon_{ave} = 2.5p \quad (2)$$

where ε_{ave} is average strain, and p is shear reinforcing bar ratio (expressed as a direct value, not in %). The displacement index is obtained by multiplying average strain ε_{ave} by member thickness

D. Based on past experimental and analysis conditions (axial force ratio and specimen dimensions), this index is applicable under the conditions that the average axial force ratio of members is 0.1 or less, and the minimum member dimension is 0.4 m. In this index, the limit state is defined as the condition where the horizontal load carrying capacity of a statically indeterminate structure is maintained, although the load carrying capacity of individual members might be slightly reduced. In other words, this index is not intended for application to statically indeterminate structures, because a decrease in the load carrying capacity of members directly leads to a decrease in the horizontal load carrying capacity of the overall structure.

4.2 Relative displacement on compressive edge in RC member

It is well known that concrete damage under uniaxial compressive stress conditions occurs locally. Experimental studies have shown that the failure zone remains within 200 mm in both cylindrical and rectangular specimens with varying height-to-width (H/D) ratios [10]. The compressive failure of concrete is often evaluated using principal compressive strain. However, since strain is greatly affected by the element size dependence in the analysis model, the limit value is set from the in-element reference length determined from the direction of the principal strain [7]. Based on the above physical phenomena and the current strain-based design concept, we verified that setting a deformation limit of 1% over a 200 mm node interval results in a more conservative (safer) design than the current design method. In other words, the relative displacement between the nodes 200 mm away from the member edge at the compressive edge of the RC member is 2 mm (200 mm multiplied by 1%), which is used as the index and limit value proposed in this study. The node positions used for the calculation are shown in Fig. 5.

$$\Delta l_{lim}' = 2.0 \quad (3)$$

where $\Delta l_{lim}'$ is the limit value of relative displacement on the compressive edge [mm]. However, the nodes used for the verification must be at least 200 mm away from the end of the member excluding the haunch. In the case of the in-plane shear failure mode, the direction of the principal compressive strain in the element may deviate by up to 45 degrees relative to the direction between the nodes. However, we have checked that even if the direction deviates by 45 degrees, setting the limit value of the index to 2 mm ensures that the evaluation remains conservative, regardless of the direction of the principal compressive strain.

Since the plasticized region in concrete is localized within the compression damage zone, other compression regions exhibit elastic deformation. Therefore, ensuring that the relative distance between the verification nodes is at least 200 mm incorporates elastic deformation, allowing for a conservative (safe-side) evaluation. In other words, no adjustments to the element dimensions are required for verification, which is a key advantage of the proposed index. The applicable conditions for this index

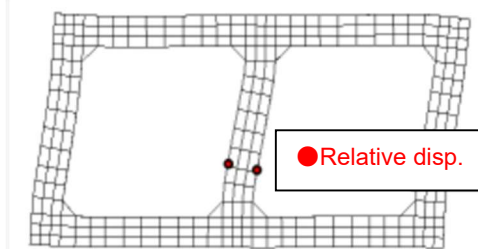


Fig. 4 Image of thickness increment of RC member

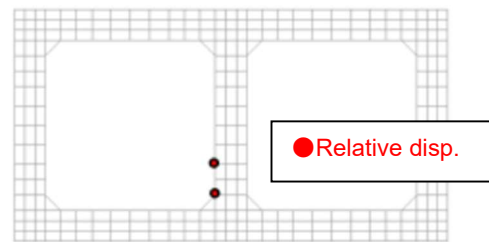


Fig. 5 Image of relative displacement on compressive edge in RC member

are the same as those of the index described in section 4.1.

5 BEHAVIOURAL ANALYSIS AND DAMAGE EVALUATION OF COLUMN MEMBERS

5.1 Comparison of analysis results and experimental results for damage to column members

The maximum principal strain results for the first-floor columns of the test structure after the seismic wave input are shown in Figs. 6, 7, and 8, and the maximum principal strain results for the entire test structure are shown in Fig. 9. As in the experiment, the damage was concentrated on the first floor, and the analysis results closely matched those of the experiment. In the experiment, the first floor columns

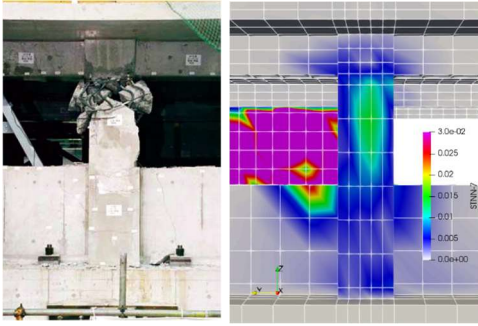


Fig. 6 Damage to the 1st floor column (X_1Y_3) and maximum principal strain

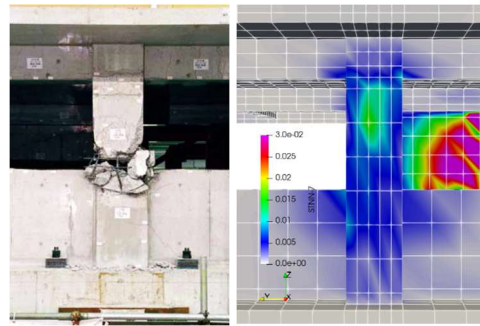


Fig. 7 Damage to the 1st floor column (X_1Y_2) and maximum principal strain

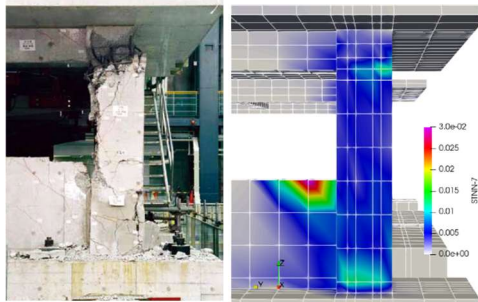


Fig. 8 Damage to the 1st floor column (X_1Y_1) and maximum principal strain

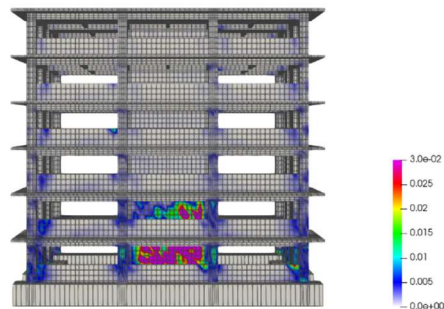


Fig. 9 Damage to the entire building (maximum principal strain)

X_1Y_2 and X_1Y_3 , which had waist walls, experienced shear failure. The analysis also revealed significant damage in the first floor columns X_1Y_2 and X_1Y_3 .

5.2 Analysis of inter-layer displacement and evaluation of damage to columns

The inter-layer displacement between the first and second layers of X-Y and Y-Z at X_2Y_1 at an amplitude magnification of 100% in the experiment and analysis is shown in Figs. 10 and 11, respectively. The analysis results showed displacement approximately 50 mm smaller than the experimental results in the Y direction, and approximately 30 mm greater in the Z direction. Although the displacement in the Z direction did not turn negative (the side where the building sinks) after damage, the overall results, including large displacement and damage during shear failure, were closely aligned with the experimental results. One possible reason why the Z-direction displacement did not turn negative is that the model used in the analysis did not fully capture the decrease in restraining force caused by cover peeling and the accompanying rebar buckling.

In the figures, the points where any of the columns exceeded the limit value for any of the displacement indices are marked with red circles. Of the total duration of 60.32 seconds, the “relative displacement on compressive edge in RC member” exceeded the limit value first at 50.30 seconds, when the amplitude ratio was 100%. From these figures, it can be observed that the index reached the limit value when the displacement in the Y direction swung to the most negative side. In the experiment,

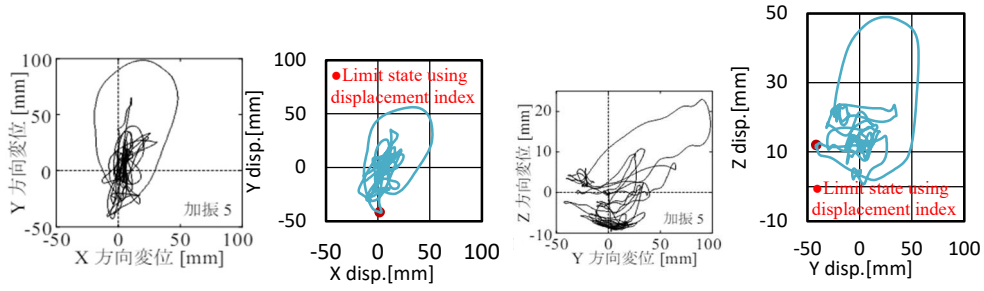


Fig. 10 Inter-layer displacement in the X-Y direction (100% amplitude)

Fig. 11 Inter-layer displacement in the Y-Z direction (100% amplitude)

the limit state was reached at an amplitude ratio of 100%, and collapse occurred at 60%. This suggests that this index can reasonably evaluate the limit state.

Figure 12 shows the minimum principal strain contour of the column where the compressive edge displacement difference reached the limit value. It can be seen that shear compression failure occurred in the column on the first floor that was evaluated. This failure is likely due to the effective reduction in the shear span ratio (a/d) to approximately 1.67, caused by the presence of the waist wall. Meanwhile, the “thickness increment of RC member” also exceeded the limit value, albeit with a delay. This occurred at two first-floor columns, X_3Y_1 and X_3Y_4 . Figure 13 shows the contours of the columns where the “thickness increment of RC member” exceeded the limit value. At the bottom of the columns, large maximum principal strains occurred due to the development of bending cracks, but the index did not reach the limit value at these locations. At the top of the columns, diagonal cracks began to develop, eventually causing the index to exceed the limit value.

The above indicates that the failure mode can also be appropriately estimated using these indices. After loading, the “relative displacement on compressive edge in RC member” exceeded the limit value in all columns. In particular, “relative displacement on compressive edge in RC member” was greater than 10 mm in more locations on X_1 Street than on X_3 Street, with concentrations in X_1Y_2 and X_1Y_3 . Thus,

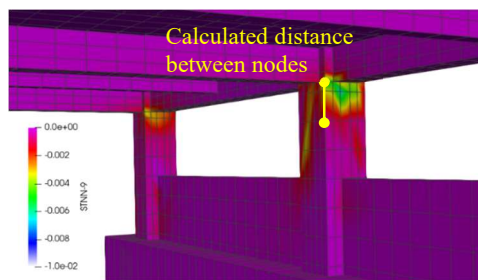


Fig. 12 Minimum principal strain of column X_1Y_2

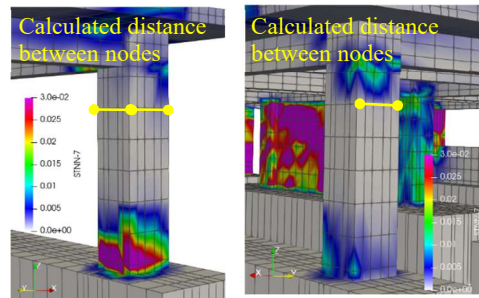


Fig. 13 Maximum principal strain (left: X_3Y_1 column, right: X_3Y_4 column)

the proposed index clearly reflects that the restraint provided by the waist wall had a significant influence on the damage to the columns.

6 CONCLUSIONS

A simulation analysis of a full-scale 6-story reinforced concrete building was conducted using nonlinear material FEM analysis, with the aim of establishing a framework for quantitatively and rationally evaluating the risk of building collapse. The following conclusions were obtained.

1. To improve the accuracy of earthquake response analysis of full-scale buildings, the influence of drying shrinkage must be properly accounted for. In this study, the simulation analysis was conducted by reducing the Young's modulus and tensile strength of concrete by 20% and 40%, respectively, from

the values calculated based on the formula in the standard specification for Concrete Structures. The results closely matched the damage patterns and inter-layer displacement observed in the experiment.

2. Although the analysis was unable to express the behaviour of the entire building sinking in the vertical direction due to damage to the columns, the inter-layer displacement after shear failure was nearly identical to the experimental results. To further enhance the accuracy of damage risk evaluation, improvements in modelling the peeling of the concrete cover and the buckling of rebar in the model should be considered.

3. Use of the proposed indices, which focus on relative deformation within structural members, enabled a quantitative and rational assessment of collapse risk, taking into account the structural redundancy of the building. Furthermore, the indices made it possible to estimate the location of damage, the degree of damage, and even the failure mode of columns.

Acknowledgements

We would like to thank Professor Nobuhiro Chijiwa (Institute of Science Tokyo) for their assistance in developing the analysis model used in this research. In addition, part of this work was supported by the Council for Science, Technology and Innovation (CSTI), Cross-ministerial Strategic Innovation Promotion Program (SIP), “Development of a Resilient Smart Network System against Natural Disasters” Grant Number JPJ012289 (Funding agency: NIED).

References

- [1] Ministry of Education, Culture, Sports, Science and Technology. 2021. *National Seismic Prediction Map 2020 Edition*.
- [2] Hashimoto, Noburu. 2021. “A photographer who covered all the major earthquakes in Japan.” Accessed June 27. <https://jbpress.ismedia.jp/articles/-/64326?page=4>
- [3] Nikkei Xtech. 2018. “Local government office buildings lagging in earthquake resistance: Can they continue to function in the event of a disaster?” Accessed February 2024. <https://xtech.nikkei.com/atcl/nxt/column/18/00251/040600006/>
- [4] Ministry of Education, Culture, Sports, Science and Technology. 2006. *Draft Report of Results: Great Earthquake Reduction Special Project in Major Cities*. II.3.2.2 Development of a Three-Dimensional Dynamic Analysis System for Full-Scale Reinforced Concrete Buildings.
- [5] Maekawa, Koichi, Amron Pimanmas, and Hajime Okamura. *Nonlinear Mechanics of Reinforced Concrete*. SPON Press, 2003.
- [6] Maekawa, Koichi, and Nobuhiro Chijiwa. Thermo-hygral case-study on full scale RC building under corrosive environment and seismic actions. *Journal of Advanced Concrete Technology*, volume 13, 2015, pp. 465-478.
- [7] JSCE Concrete Committee. “English Summary Edition of JSCE Standard Specifications for Concrete Structures. 2017.” Accessed February 8. <https://www.jsce.or.jp/committee/concrete/event/Summary%20edition-JSCE%20standard%20specifications%20for%20concrete%20structures20240227-PW.pdf>
- [8] JSCE Committee on the Nuclear Civil Engineering. “JSCE SEISMIC PERFORMANCE VERIFICATION GUIDELINES FOR CRITICAL UNDERGROUND REINFORCED CONCRETE STRUCTURES IN NUCLEAR PLANTS -2021- DRAFT.” Accessed February 8. <https://committees.jsce.or.jp/ceofnp/system/files/Guidelines2021DRAFT20230804.pdf>
- [9] Komatsu, Satoshi, Yoshinori Miyagawa, Toyofumi Matsuo, Akihito Hata, Tsuguhiro Shimabata and Hikaru Nakamura. 2023. “Applicability of Deformation Indices Reasonably Evaluating Load Carrying Capacity and Failure Mode of Full-Scale RC Members Subjected to Bilateral Loads.” *Journal of Advanced Concrete Technology* Vol. 21, pp. 421-435. doi:10.3151/jact.21.421.
- [10] Lertsrisakulrat, Torsak, Ken Watanabe, Maki Matsuo, and Junichiro Niwa. 2001. “Experimental study on parameters in localization of concrete subjected to compression.” *Journal of Materials, Concrete Structures and Pavements, JSCE*, 669/V-50, 309-321. doi:10.2208/jscej.2001.669_309.